Penerbit Akademia Baru

Journal of Research in Nanoscience and Nanotechnology

Journal homepage:
http://akademiabaru.com/submit/index.php/jrnn/index
ISSN: 2773-6180

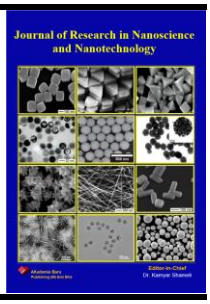

Poly Lactic-*co*-Glycolic Acid Nanoparticles: Flow Rates and Gauge Sizes Influence the Droplet Surface Tension and Particle Sizing

Adibah Shakri[1], Muhammad Ayman Ikmal Shawaludin[1], Izzat Fahimuddin Mohamed Suffian[2], Irna Farikhah[3], Khairunnisa Mohd Pa'ad[1,*]

[1] Department of Chemical and Environmental Engineering, Malaysia-Japan International Institute of Technology, Universiti Teknologi Malaysia, 54100 Kuala Lumpur, Malaysia
[2] Department of Pharmaceutical Technology, Kulliyyah of Pharmacy, International Islamic University Malaysia, 25200 Kuantan, Pahang, Malaysia
[3] Department of Mechanical Engineering, University of PGRI Semarang, Semarang, Indonesia
* Correspondence: khairunnisa.kl@utm.my
https://doi.org/10.37934/jrnn.9.1.112

ABSTRACT

Electrospray is a novel and versatile approach to the synthesis of nanosized particles. In this paper, the effects of electrospray process parameters such as gauge size (18 G-25 G) and flow rate (0.9-1.5 ml hr^{-1}) on droplet surface tension and electrospray particle size were evaluated. 25 mg Poly Lactic-*co*-Glycolic Acid (PLGA) were dissolved in 100 ml acetone before being subjected to electrospray. Tate's Law was used to calculate the surface tension while the Malvern nanosizer was used to measure the particle size. Based on Tate's Law calculation, when the gauze size increased from 18 G-25 G, the droplet surface tension increased from 10.07 Nm^{-1} to 18.17 Nm^{-1} showing a direct pattern. At the same time, the flowrate is inversely proportional to droplet surface tension. When the flow rate increased from 0.9-1.5 ml hr^{-1}, the droplet surface tension was reduced. This is due to the increasing ratio of vicious force and surface tension. For particle size, as surface tension increased from 10.07 Nm^{-1} to 18.17 Nm^{-1}, particle size increased from 205.57 nm to 612 nm owing to the corona discharge producing larger progeny droplets that chain into smaller particles through coulomb fission as more charge is required to overcome the surface tension. In conclusion, flow rate and gauge size influenced the surface tension thus affecting the nanosized particles.

Keywords:
Electrospray, nanomaterials, Tate's law, PLGA

Received: 16 Aug. 2023 | **Revised: 27 Sep. 2023** | **Accepted: 21 Nov. 2023** | **Published: 7 Dec. 2023**

1. Introduction

PLGA stands out as an incredibly versatile polymer due to its excellent biocompatibility and biodegradability [1]. It has been approved by the U.S. Food and Drug Administration (FDA) for numerous clinical uses, especially in drug delivery, offering sustained release properties. Moreover,

leveraging PLGA as a nanocarrier has demonstrated significant enhancements in the bioavailability of therapeutic agents across various biomedical applications [2]. Nanoparticle synthesis with uniformly controlled particle size can be used in various applications including industrial; sensors and catalysts [3,4], medical and nutraceutical. Hence, several methods such as emulsification, nanoprecipitation, spray drying and many more have been implemented to obtain desirable nanosized particles. However, conventional methods such as emulsification and nanoprecipitation require extreme conditions, large amounts and harmful chemicals as solvents, making them costly and inefficient [5,6]. On the other hand, electrospray provides a viable alternative to said conventional methods which is simpler and more versatile for the synthesis of nanoparticles. In addition, the electrospray method has been shown to synthesise uniform, stable [7] and better controlled particle sizes [8]. Generally, solution and process parameters play important roles in optimizing the best output and desirable nanoparticles [9,10]. Similar to other methods, electrospray is highly dependent on its process parameters such as nozzle size, flowrate, molecular weight and choice of solvent to produce smaller nanosized particles [11]. Electrosprays employ the use of electrical charge to a liquid through a nozzle, leading to the formation of a small droplet of different sizes ranging from micrometres (μ) to nanosized (nm) particles. High voltage power is supplied to the nozzle, and the liquid that passes through the nozzle is highly electrified and distorted into a conical shape commonly known as a Taylor cone (Figure 1).

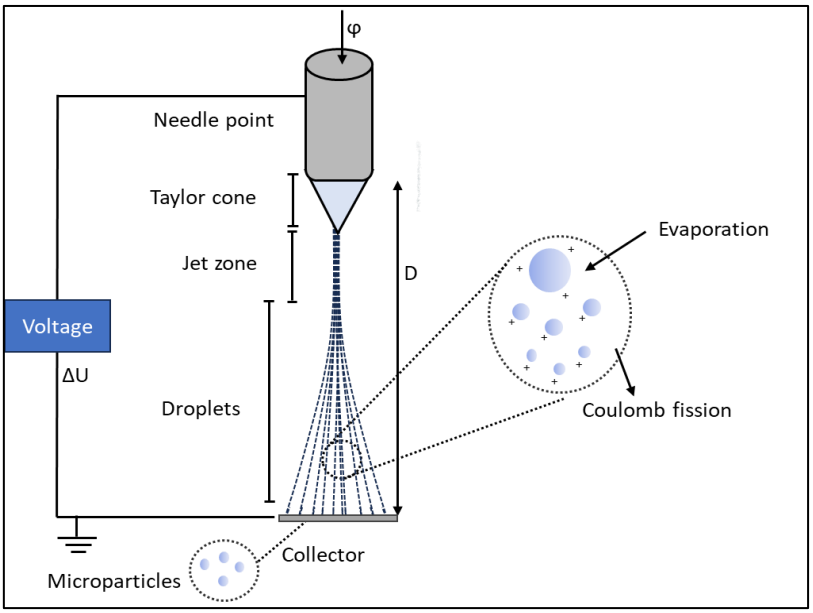

Fig. 1. Schematic diagram of the Electrospray process to form a stable Taylor cone jet formation
Flowrate (ϕ), potential difference (ΔU) and working distance (D).
Adapted from Morais *et al.*, [12]

The mechanism occurs when the electrostatic forces overcome the surface tension of the droplets indicating that surface tension significantly influences the production of particles [13]. The surface tension of the droplet is one of the major forces of the mechanism of the electrospray synthesis as the droplet surface tension acts against the electrostatic force before it begins to form a Taylor-cone jet to emit droplets [14]. The surface tension of the droplet can be determined using Tate's law. Tate's law suggests that if the liquid is allowed to be dripped from the tip and form a droplet, the droplet's weight is equal to the force exerted by surface tension [15].

Typically, surface tension is manipulated by changing the concentration of the mixture subjected to the electrospray, by increasing the concentration and viscosity of the liquid, the surface tension decreases, resulting in larger particles [14]. However, the surface tension of the liquid can also be changed with the manipulation of the process parameters (eg; flow rates and needle gauze size) of the electrospray set-up. Moreover, previous studies showed the direct relationship of process parameters with the formed nanoparticle size which limited knowledge of its relation to the droplet surface tension. Therefore, varying mixture concentration to achieve higher surface tension can be limited under the process parameters which resulted in inconsistency of particle size formed in the past. Hence, in this study, varying needle gauge sizes and flowrates of electrospray will be used to synthesize the nanoparticle to understand the overlying mechanism of the droplet surface tension to the formation of electrospray particle size. The performance of the electrospray can be evaluated by the effects of the flowrate and needle gauge size to achieve smaller particle sizes. Tate's Law Procedure was employed to evaluate the surface tension of the different parameters of 18- 25 G needle gauge size and 0.9-1.5 ml hr^{-1} flowrate. An electrospray was then set up for the analysis of the particle size effect on surface tension with similar parameters at a constant voltage of 7.5 kV.

2. Materials and Methods

2.1 Materials

The biodegradable polymer PLGA (65/35 DL-lactide/glycolide copolymer) with a molecular weight between Mw 40,000-75,000 g mol^{-1} was purchased from Sigma Aldrich, USA. Acetone with a purity of 98% was purchased from R&M Chemicals, Malaysia. Both materials used were taken directly without any further purification or treatment. Tween 80 with a purity of 98% was purchased from Merck, Darmstadt, Germany and a stock solution of 0.2% Tween 80 was prepared with deionised water prior used.

2.2 Drop Weight Method

The effects of the needle gauge size and flowrate on the droplet surface tension were evaluated using a modified Tate's law procedure adopted from Giagino *et al.*, [10]. Briefly, 25 mg PLGA polymer was prepared using 100 ml of acetone as a solvent and stirred (MS-MP, Daihan Scientific, Singapore) at 350 rpm for 30 minutes to obtain yellowish coloured solution. The PLGA solution was filled into a 5 mL syringe attached to a tubing and blunt end needle. The liquid was dripped at a deposition distance of 5 cm from the experimental set-up in Figure 2. The surface tension was calculated using Eq. (1) [16] where τ is the surface tension (Nm^{-1}), mg is the mass of the droplet and d is the outer diameter of the needle. Eq. (2) is derived from Eq. (1) as the average mass of a single drop will be equal to $m = (M_f - M_i)/N$ where M_f is the mass of the petri dish with drops (g), M_i is the empty petri dish (g) and N is the number of drops produced. Experiments were conducted with varying flow rates (0.9, 1.2 and 1.5 ml hr^{-1}) and gauge sizes (18, 21, 23 and 25 G) as listed in Table 1.

$$\tau = \frac{mg}{\pi d} \quad (1)$$

$$\tau = \frac{(M_f - M_i)g}{\pi d N} \quad (2)$$

Table 1. Formulation parameters that was used to determine surface tension and to prepare PLGA nanoparticles

Flowrate, ml hr^{-1}	Needle Gauge Size, G	Internal diameter (ID), mm	Outer diameter (OD),mm
0.90	18	0.84	1.27
1.20	21	0.51	0.82
1.50	23	0.34	0.64
	25	0.26	0.50

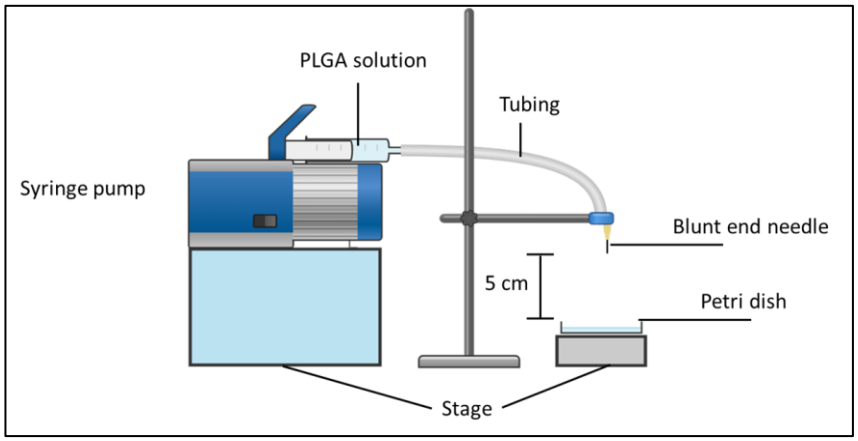

Fig. 2. Schematic diagram for surface tension measurements using Tate's Law procedure

2.3 Preparation of PLGA Nanoparticles

PLGA nanoparticles were prepared by the electrospray method and the schematic diagram of the electrospray setup was illustrated in Figure 3. Electrospray setup consists of several components; the syringe to hold the PLGA solution, the syringe pump, the particles collector and the voltage supply to the system. The constant conditions of the electrospray setup are as follows; Starting solution of 5 mL, a tubing (TYGOPRENE™ TYGON XL-60, Darwin Microfluids, France) with a length of 10 cm connecting the syringe (Terumo Europe N.V, Belgium) and the needle (Darwin Microfluids, France), a 5 cm needle tip to petri dish (100 mm x 15 mm able to hold approximately 20 mL liquid) distance and voltage supplied (PS35-PV, Nanolab Instruments, Malaysia) of 7.5 kV to the electrospray based on preliminary study that showed stable Taylor Cone Jet formation at particular voltage. The tubing was specifically chosen from Saint-Goban performance plastics that are compatible with most chemicals especially one that has good compatibility with acetone that was used in this study.

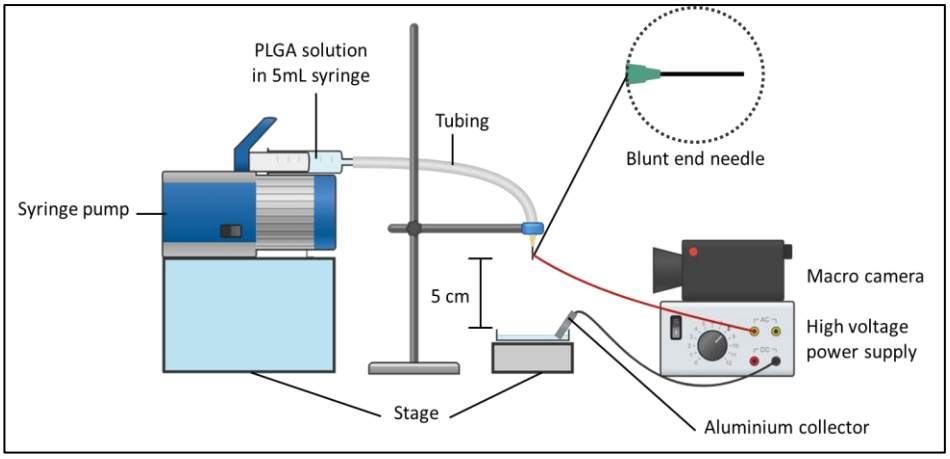

Fig. 3. Schematic diagram of electrospray setup to synthesis PLGA nanoparticles

Briefly, PLGA polymer was prepared similarly to the drop weight method. The PLGA solution was filled into a 5 mL syringe attached to a tubing and blunt end needle at different gauge sizes as listed in Table 1. Then, the syringe was positioned on top of the syringe pump (NSL-20, Nanolab Instrument, Malaysia) and the tip of the needle was connected to the high voltage power supply while a grounded electrode was connected to the aluminium collector (20 mm x 10 mm) immersed in the glass a petri dish containing a collection medium of 20 ml of 0.2 % Tween 80. The PLGA solution was sprayed over at different flow rates as listed in Table 1 inside a chamber (200 cm x 100 cm) at room temperature of 25 °C and a relative humidity of 66 %. A digital camera (X4, Shenzen Haiweixun Electronics Co. Ltd, China) was used to ensure the Taylor cone jet formation. Finally, the PLGA nanoparticles were collected in the glass petri dish and were kept in a 15 ml centrifuge tube at 4 °C prior to use.

2.4 Particle Size Measurements

The particle size of all the PLGA nanoparticles synthesis using different flow rates and needle gauge sizes were measured with a particle size analyzer (Nano-ZS90, Malvern Instruments Co. LTD, UK) at a scattering angle of 90° and at room temperature. PLGA nanoparticles were prepared at a dilution factor of 1:1000 with deionised water. 1 mL of prepared PLGA nanoparticles was added to the clean cuvette and small bubbles were eliminated using pipette tips to ensure uniform dispersion of nanoparticles.

3. Results and Discussion

3.1 Effect of Flow Rate and Gauge Size on Droplet Surface Tension

Three concentrations of flowrates (0.9, 1.2, and 1.5 ml hr^{-1}) and four different gauge sizes (18, 21, 23 and 25) were used to evaluate the surface tension. The effects of the flowrates and gauge size on the surface tension were plotted in Figure 4. Figure 4 (a) shows as the flowrates increased from 0.9 – 1.5 ml hr^{-1}, the surface tension was reduced in all gauge sizes indicating an inversely proportional trend between flowrate to surface tension. In 25 G, with the smallest internal diameter size of 0.26 mm, the biggest surface tension drops of approximately 3.63 were observed from 18.17 ^{1} to 14.54 Nm^{-1} while at 18 G, with the biggest internal diameter of 0.84 mm, showed the smallest surface tension

dropped from 11.30 to 10.07 Nm^{-1}. As higher flow rates will result in higher surface tension, higher voltage is needed to overcome the surface tension [17] but, in this situation, the voltage was maintained constant at 7.5 kV. The flowrates act directly on the liquid to overcome the surface tension to produce the droplet and may cause a change in the dynamic viscosity and characteristic velocity of the fluid in the needle, where the flowrate affects the ratio of viscous forces and surface tension forces in which an increment of flowrate, in turn, reduces the surface tension of the droplet [18]. Thus, at constant voltage, a higher flow rate will cause a reduction in surface tension because of the dynamic changes in the liquid characteristics.

Figure 4 (b) shows the directly proportional trend between gauge size and surface tension. As needle gauge size increases from 18 G to 23 G (the internal diameter becomes smaller; 0.84-0.26 mm), the surface tension increases and peaks at 15.64 and 15.2 Nm^{-1} but declines past 23 G at flowrate 1.2 and 1.5 ml hr^{-1} while at 0.9 ml hr^{-1}, the surface tension shows steady increase up to 25 G. This indicates that, at 25 G gauge size (smallest diameter of 0.26 mm), the reduction of surface tension only happened at 1.2 and 1.5 ml hr^{-1} flow rates. Based on Tate's Law, prior to the droplet breakage, the weight of the droplet is equal to the opposing force of the surface tension. The surface tension is inversely proportional to the square root of the needle's radius indicating that smaller needle size corresponds to large surface tension [15].

The drop in surface tension past 23 G for the 1.2 and 1.5 hr^{-1} flowrate can be attributed to the critical size of the needle. At 25 G, the formation of the droplets does not even lead to a drop in the surface tension. But when the critical size is passed, the droplet maintains its shape resulting in higher meniscus stability, which can increase the capacity of the droplet to retain and accumulate mass [18] that relates to the basis of Tate's Law which indicates higher mass correlates to an increased in surface tension.

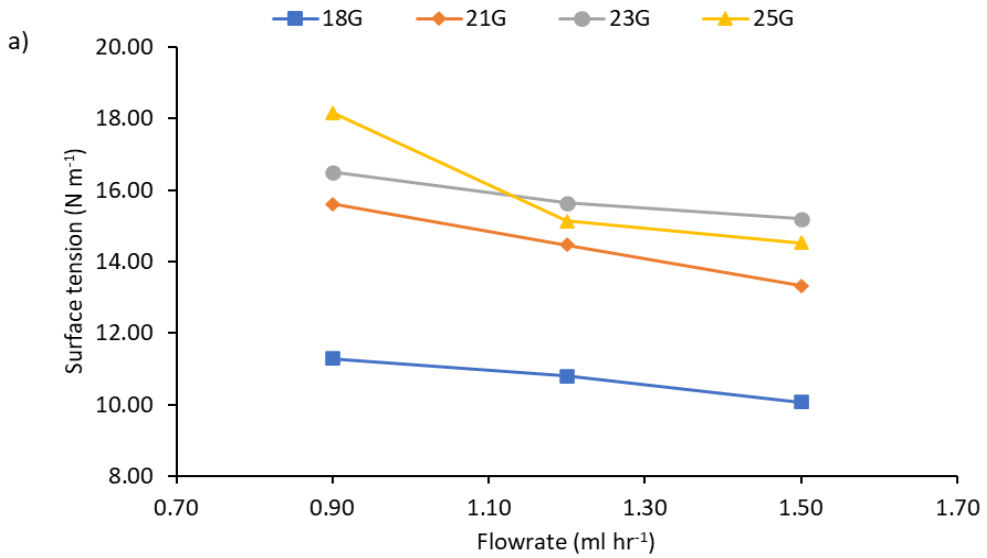

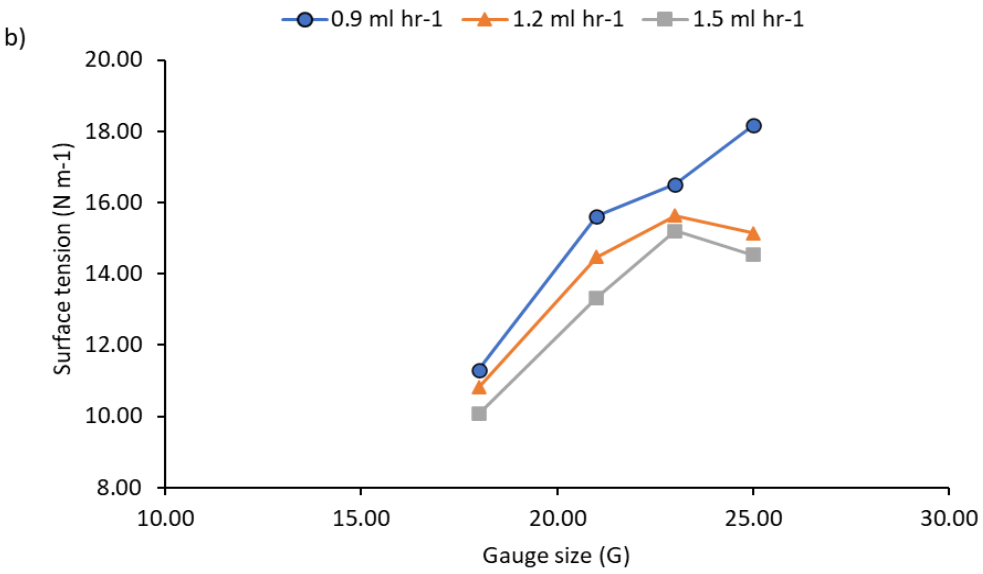

Fig. 4. a) The effects of flowrates on the surface tension, and b) the effects of different gauge sizes on surface tension

3.2 Effect of Flow Rate and Gauge Size on Particle Size

Figure 5 (a) depicts that with the increase of flowrates from 0.9 to 1.5 ml hr^{-1}, the particle size was reduced. Usually, higher flowrates will result in higher particle sizes due to the higher volume of solvent that did not fully evaporate during the electrospray process [19]. However, other factors such as solution concentrations and the deposition distance can also cause the evaporation process [20]. The reduction of the particle size with increasing flowrates can be attributed to the reduction of viscous forces in the droplet.

Based on the study of Alberini *et al.*, 2017, Reynold numbers can be evaluated using the equation of

$$\mathrm{Re} = \frac{\rho_c u d}{\mu_c}$$

where ϱ_c is the density of continuous phase (kgm^{-3}), u is the velocity of the water flow, d is the diameter of needle drop and μ_c is the viscosity of the fluid. Higher flowrates correspond to higher Reynolds numbers [18] which reduces the viscosity forces. So, when the flow rates increase, the Reynold numbers increase which lowers the viscosity which could affect the reduction in particle size [7]. In addition, low viscosity corresponds to a low concentration of particles in a solution. A study by Tanaka et al., demonstrates the effects of PLGA concentration on the formed PLGA nanoparticles. In this study, low concentration equals to the ratio between 0.5 to 2 while high concentration is more than the ratio of 4 from the initial concentration of PLGA used [21]. Furthermore, there is the possibility of a transition phase of electrospray (particle) to electrospinning (fibre) at a higher concentration of 5 mg w/w that contributes to denser and bigger particle size [22]. Figure 6 illustrates the possible mechanism of the PLGA nanoparticle formation based on the solution viscosity.

Figure 5 (b) presents the effects of different gauge sizes on particle size. As the gauge size increased, the particle size also increased indicating a directly proportional trend regardless of any flowrates. At 25 G, where the internal diameter of the needle is the smallest at 0.26 mm, the particle size was reduced indicating that the particle size will be influenced by a particular needle diameter.

Needle size has a direct relationship with the particles produced. Similarly, the finding by Anani *et al.,* [23] illustrated that 27 G needle size is better performance compared to 21 G. As in this study, 25 G was used instead of 27 G, and as a comparison 25 G is better than 23 G which produced 459.40 nm than 521. 06 nm.

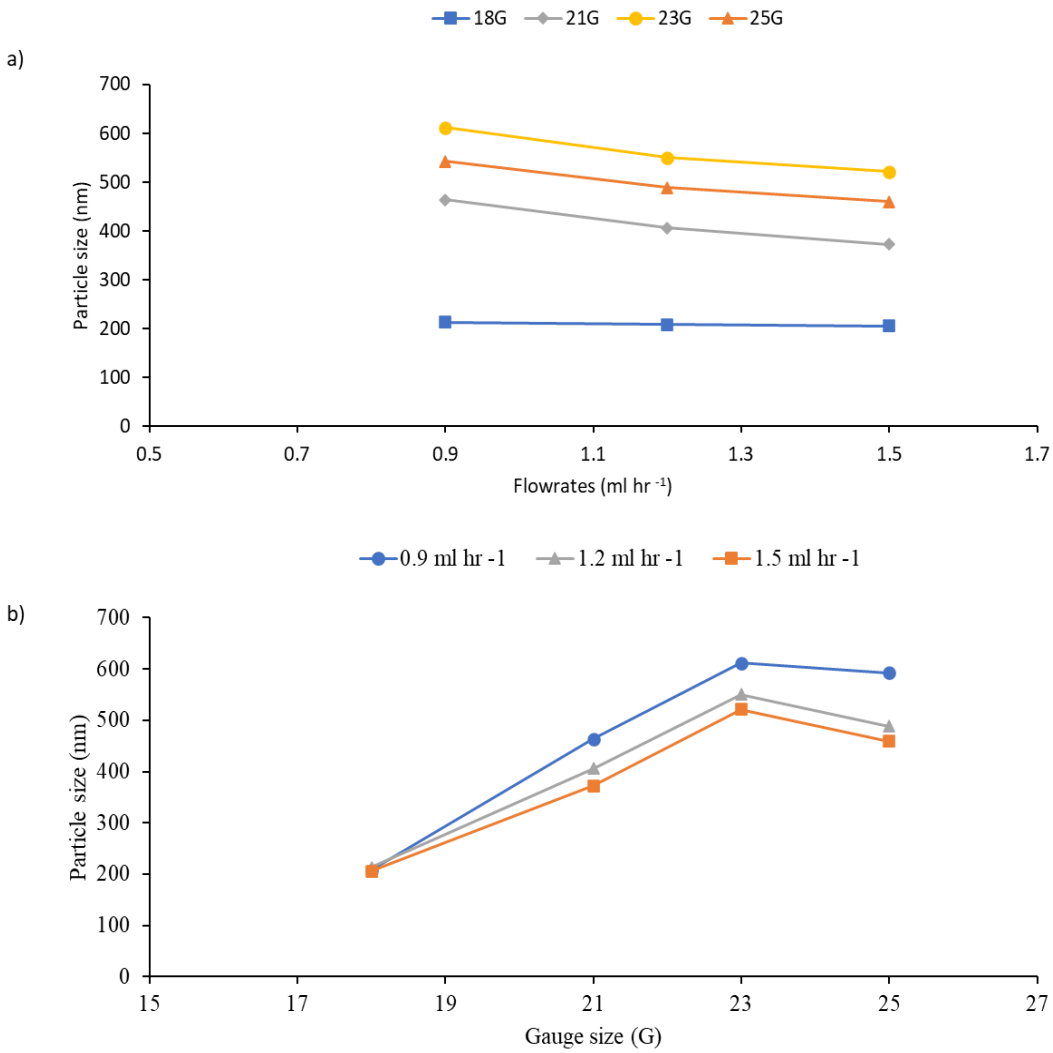

Fig. 5. a) The effects of flowrates on the particle size, and b) the effects of different gauge size on particle size

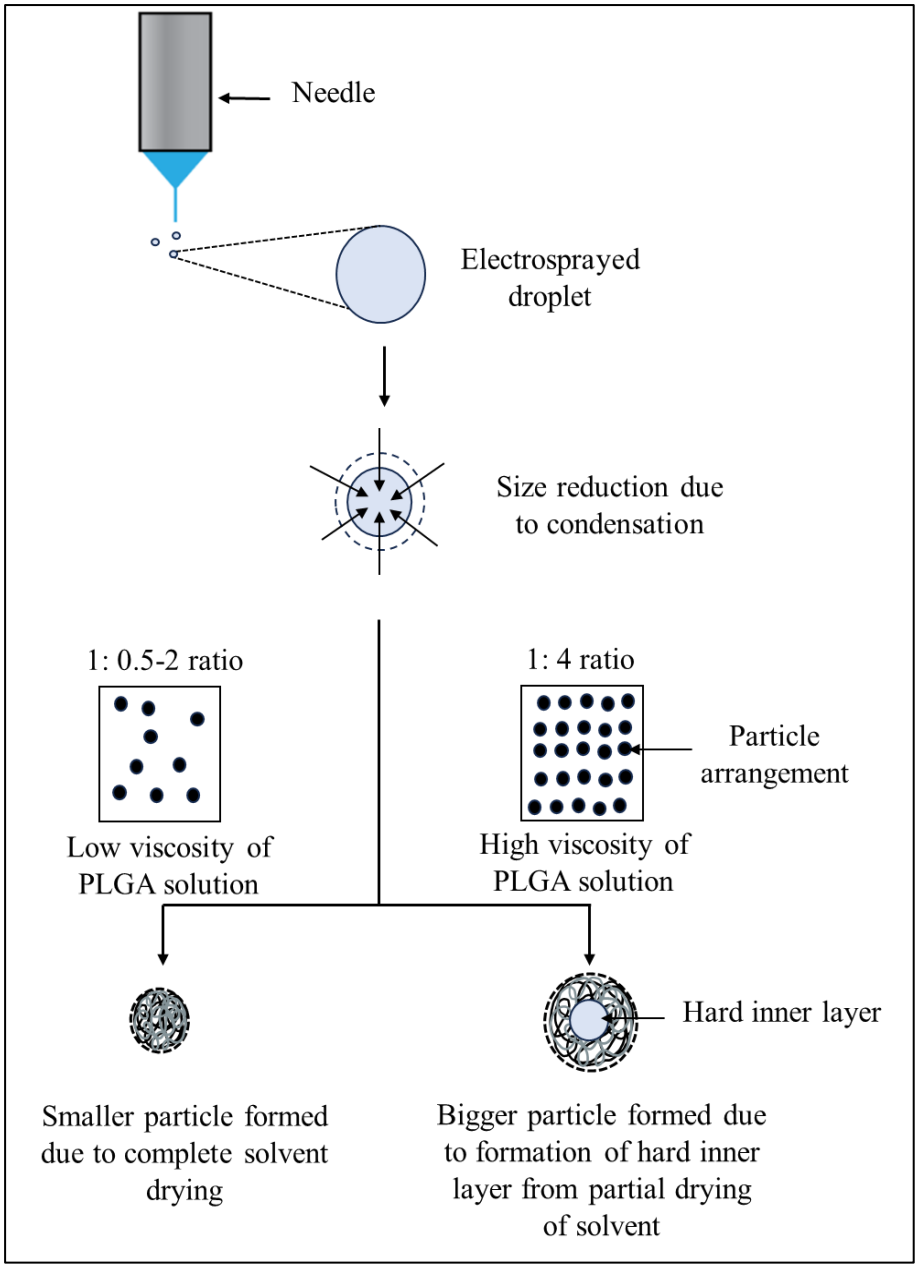

Fig. 6. Schematic illustration of the mechanism of PLGA nanoparticle formation

3.3 Relationship of Surface Tension and Particle Size

Figure 7 illustrates the relationship between the surface tension and particle size. Based on Figure 7, it can be observed that the particle size showed a linear trend with slight fluctuations when surface tension is increased due to the electrohydrodynamic forces acting upon the Taylor Cone-jet. This occurrence involves two primary forces on the droplet; the electric current acting as a driving force and the opposing surface tension. A Taylor Cone jet is formed when the electric current supplied surpasses the surface tension. Ionization leads to the production of larger progeny droplets when there is less current available for diffusion. As a result, higher surface tension tends to generate a corona discharge that forms larger sized droplets [24,25]. However, at the highest surface tension of 18.17 Nm^{-1}, the fluctuation happened showing a decrease in the particle size from 612.0 nm to 592.2 nm and at 15.61 Nm^{-1} that caused particle size to reduce from 521.06 nm to 463.80 nm. Both

fluctuations happened at different gauge size in which suggest a few possibilities such as a momentary perturbation in spindle spraying modes observed at 25G (smallest diameter), that may have been caused by repulsive action. Spindle spraying modes are known to yield smaller particle sizes due to its shearing characteristics which may reduce the resisting interfacial forces (surface tension). Additionally, a Taylor Cone Jet can shift partly due to a varicose instability from the increased surface tension that may have affected the droplet size [26]. Moreover, a complex jetting behaviour with a shorter meniscus could have also contributed to the smaller particles, resulting in unpredictable particle size [27].

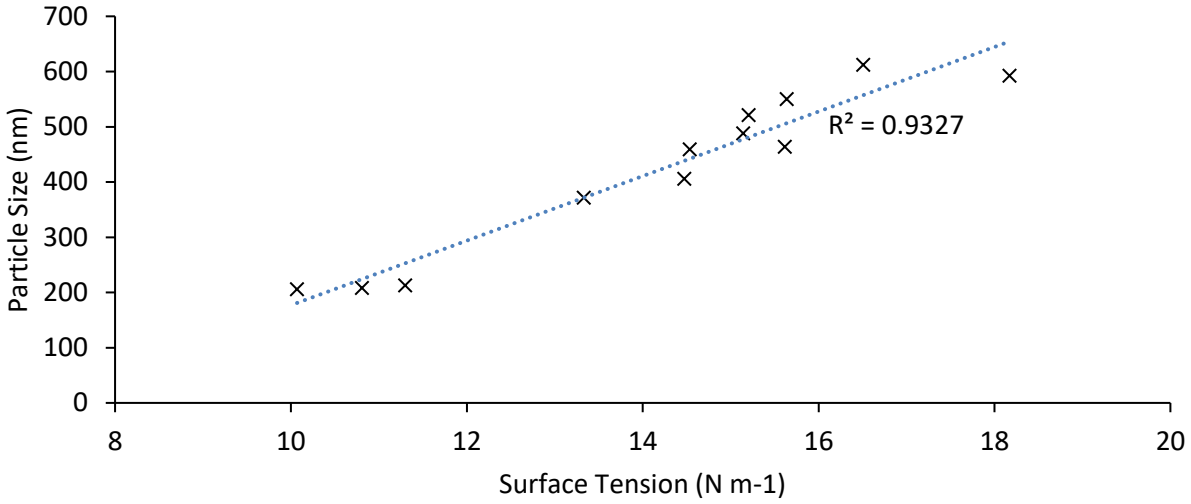

Fig. 7. Relationship between surface tension and particle size

4. Conclusions

In conclusion, the process parameters especially flowrates needle size influence the droplet surface tension and the particle size of PLGA nanoparticles. Higher flowrates will reduce the surface tension at constant voltage supplied due to dynamic changes in liquid characteristics while the gauge sizes only reduce the surface tension at particular sizes of 25 G with the smallest diameter and at certain flowrates of 1.2 and 1.5 ml hr^{-1}. As for particle size, both flowrates and gauge sizes do influence the particle size produced as higher flowrates will produce bigger particle sizes regardless of gauge size due to the possibility of the increase in Reynold numbers. While at particular sizes of 25 G with the smallest size diameter, smaller particle size was produced. Based on this research, a relationship between surface tension and particle size can be deduced as the higher the surface tension, the bigger the particle size formed.

Funding

This research was funded by the Ministry of Higher Education, Malaysia through the Fundamental Research Grant Scheme for Research Acculturation of Early Career Researchers no FRGS-RACER/1/2019/SKK15/UIAM//1. The authors acknowledge the financial support from Malaysia - Japan International Institute of Technology (MJIIT), Universiti Teknologi Malaysia for sponsoring her PhD studies.

References

1. Zhang, Dan, Lin Liu, Jian Wang, Hong Zhang, Zhuo Zhang, Gang Xing, Xuan Wang, and Minghua Liu. "Drug-loaded PEG-PLGA nanoparticles for cancer treatment." *Frontiers in Pharmacology* 13 (2022): 990505. https://doi.org/10.3389/fphar.2022.990505
2. Chatterjee, Manosree, and Nripen Chanda. "Formulation of PLGA nano-carriers: specialized modification for cancer therapeutic applications." *Materials Advances* 3, no. 2 (2022): 837-858. https://doi.org/10.1039/D1MA00600B
3. Suhaimi, Mohd Husairi Fadzilah, Nur Arfah Natasyah Ambo, Akmal Lutfi, Izzah Nur Zulaikha Masjhur Masjhur, Kevin Alvin Eswar, Jalal Rouhi, and Muhammad Rusop Mahmood. "Fabrication of ZnO Nanostructures Doped with Nb at Different Concentration as a Argon Sensor." *Journal of Advanced Research in Applied Sciences and Engineering Technology* 31, no. 1 (2023): 365-372. https://doi.org/10.37934/araset.31.1.365372
4. Nandiyanto, Asep Bayu Dani, Brigitta Stacia Maharani, and Risti Ragaditha. "Calcium Oxide Nanoparticle Production and its Application as Photocatalyst." *Journal of Advanced Research in Applied Sciences and Engineering Technology* 30, no. 3 (2023): 168-181. https://doi.org/10.37934/araset.30.3.168181
5. Rane, Ajay Vasudeo, Krishnan Kanny, V. K. Abitha, and Sabu Thomas. "Methods for synthesis of nanoparticles and fabrication of nanocomposites." In *Synthesis of inorganic nanomaterials*, pp. 121-139. Woodhead Publishing, 2018. https://doi.org/10.1016/B978-0-08-101975-7.00005-1
6. Hernández-Giottonini, Karol Yesenia, Rosalva Josefina Rodríguez-Córdova, Cindy Alejandra Gutiérrez-Valenzuela, Omar Peñuñuri-Miranda, Paul Zavala-Rivera, Patricia Guerrero-Germán, and Armando Lucero-Acuña. "PLGA nanoparticle preparations by emulsification and nanoprecipitation techniques: Effects of formulation parameters." *Rsc Advances* 10, no. 8 (2020): 4218-4231. https://doi.org/10.1039/C9RA10857B
7. Castillo, Eduardo A., Ranganathan Kumar, and Aravinda Kar. "Silver nanoparticle electrospray laser deposition for additive manufacturing of microlayers on rigid or flexible substrates." In *Dimensional Optical Metrology and Inspection for Practical Applications VII*, vol. 10667, pp. 110-115. SPIE, 2018.
8. Faizal, Ferry, M. P. Khairunnisa, Shunichiro Yokote, and I. Wuled Lenggoro. "Carbonaceous nanoparticle layers prepared using candle soot by direct-and spray-based depositions." *Aerosol and Air Quality Research* 18, no. 4 (2018): 856-865. https://doi.org/10.4209/aaqr.2017.10.0426
9. Nur Haslinda Mohamed Muzni, Ervina Efzan Mhd Noor, and Mohd Mustafa Al-Bakri Abdullah. 2023. "Influence of TiO2 and Al2O3 Nanoparticles Addition on Thermal, Wettability and IMC Growth of Sn-3.0Ag-0.5Cu Lead-Free Solder at Different Reflow Temperature". *Journal of Advanced Research in Fluid Mechanics and Thermal Sciences* 109 (1):188-95. https://doi.org/10.37934/arfmts.109.1.188195
10. Manjunatha Swamy Kumathi Math, and Manjunath Huruli. 2023. "Impact of Al2O3 With Different Injection Pressures Using Deccan Hemp Oil Methyl Ester-Diesel Blend: An Experimental Study". *Journal of Advanced Research in Fluid Mechanics and Thermal Sciences* 107 (2):133-49. https://doi.org/10.37934/arfmts.107.2.133149
11. Vu, Linh Viet Nguyen. "Electrospray method: processing parameters influence on morphology and size of PCL particles." *Vietnam Journal of Science and Technology* 55, no. 1B (2017): 209. https://doi.org/10.15625/2525-2518/55/1B/12110
12. Morais, Alan ÍS, Ewerton G. Vieira, Samson Afewerki, Ricardo B. Sousa, Luzia MC Honorio, Anallyne NCO Cambrussi, Jailson A. Santos *et al.*, "Fabrication of polymeric microparticles by electrospray: the impact of experimental parameters." *Journal of functional biomaterials* 11, no. 1 (2020): 4. https://doi.org/10.3390/jfb11010004
13. Kageyama, Ami, Akira Motoyama, and Mitsuo Takayama. "Influence of solvent composition and surface tension on the signal intensity of amino acids in electrospray ionization mass spectrometry." *Mass Spectrometry* 8, no. 1 (2019): A0077-A0077. https://doi.org/10.5702/massspectrometry.A0077
14. Shanaghi, Elaheh, Mahdi Aghajani, Fariba Esmaeli, Mohammad Ali Faramarzi, Hoda Jahandar, and Amir Amani. "Application of electrospray in preparing solid lipid nanoparticles and optimization of

nanoparticles using artificial neural networks." *Avicenna Journal of Medical Biotechnology* 12, no. 4 (2020): 251.

15. Soni, Marshal. "A simple laboratory experiment to measure the surface tension of a liquid in contact with air." *Journal of Pharmacognosy and Phytochemistry* 8, no. 2 (2019): 2197-2202.
16. Gianino, Concetto. "Measurement of surface tension by the dripping from a needle." *Physics Education* 41, no. 5 (2006): 440. https://doi.org/10.1088/0031-9120/41/5/010
17. Surib, Nur Atiqah, and Khairunnisa Mohd Paad. "Electrospray flow rate influenced the sized of functionalized soot nanoparticles." *Asia-Pacific Journal of Chemical Engineering* 15, no. 3 (2020): e2417. https://doi.org/10.1002/apj.2417
18. Alberini, Federico, Davide Dapelo, Romain Enjalbert, Yann Van Crombrugge, and Mark JH Simmons. "Influence of DC electric field upon the production of oil-in-water-in-oil double emulsions in upwards mm-scale channels at low electric field strength." *Experimental Thermal and Fluid Science* 81 (2017): 265-276. https://doi.org/10.1016/j.expthermflusci.2016.10.023
19. Abyadeh, Morteza, Ali Akbar Karimi Zarchi, Mohammad Ali Faramarzi, and Amir Amani. "Evaluation of factors affecting size and size distribution of chitosan-electrosprayed nanoparticles." *Avicenna journal of medical biotechnology* 9, no. 3 (2017): 126.
20. Jagdale, Gargi S., Myung-Hoon Choi, Natasha P. Siepser, Soojin Jeong, Yi Wang, Rebecca X. Skalla, Kaixiang Huang, Xingchen Ye, and Lane A. Baker. "Electrospray deposition for single nanoparticle studies." *Analytical Methods* 13, no. 36 (2021): 4105-4113. https://doi.org/10.1039/D1AY01295A
21. Tanaka, Moe, Ayaka Ochi, Aiko Sasai, Hiroyuki Tsujimoto, Hitomi Kobara, Hiromitsu Yamamoto, and Akihiro Wakisaka. "Biodegradable PLGA Microsphere Formation Mechanisms in Electrosprayed Liquid Droplets." *KONA Powder and Particle Journal* 39 (2022): 251-261. https://doi.org/10.14356/kona.2022018
22. Barbero-Colmenar, Elena, Mariangela Guastaferro, Lucia Baldino, Stefano Cardea, and Ernesto Reverchon. "Supercritical CO2 Assisted Electrospray to Produce Poly (lactic-co-glycolic Acid) Nanoparticles." *ChemEngineering* 6, no. 5 (2022): 66. https://doi.org/10.3390/chemengineering6050066
23. Anani, Joshua, Hussien Noby, Abdelrahman Zkria, Tsuyoshi Yoshitake, and Marwa ElKady. "Monothetic analysis and response surface methodology optimization of calcium alginate microcapsules characteristics." *Polymers* 14, no. 4 (2022): 709. https://doi.org/10.3390/polym14040709

22. Hussain, Mohamed Hasaan, Noor Fitrah Abu Bakar, Kim-Fatt Low, Ana Najwa Mustapa, Fatmawati Adam, Mohd Nazli Naim, and I. Wuled Lenggoro. "Growth-controlled synthesis of polymer-coated colloidal-gold nanoparticles using electrospray-based chemical reduction." *Particuology* 57 (2021): 72-81. https://doi.org/10.1016/j.partic.2020.12.004
23. Nauman, Saad, Gilles Lubineau, and Hamad F. Alharbi. "Post processing strategies for the enhancement of mechanical properties of enms (Electrospun nanofibrous membranes): A review." *Membranes* 11, no. 1 (2021): 39. https://doi.org/10.3390/membranes11010039
24. Kim, Ji Yeop, Sang Ji Lee, and Jung Goo Hong. "Spray Mode and Monodisperse Droplet Properties of an Electrospray." *ACS omega* 7, no. 32 (2022): 28667-28674. https://doi.org/10.1021/acsomega.2c04002
25. Yang, Tong, Xinyu Li, Bo Yu, and Cheng Gong. "Design and Print Terahertz Metamaterials Based on Electrohydrodynamic Jet." *Micromachines* 14, no. 3 (2023): 659. https://doi.org/10.3390/mi14030659